Signal Processing 140 (2017) 1–11

Contents lists available at ScienceDirect

Signal Processing

journal homepage: www.elsevier.com/locate/sigpro

Minimum error rate detection: An adaptive bayesian approach

A. Boudjellal[a,*], K. Abed-Meraim[a], A. Belouchrani[b], Ph. Ravier[a]

[a] PRISME Laboratory, University of Orléans, 12 Rue de Blois, Orléans 45067, France
[b] EE Dept./LDCCP, Ecole Nationale Polytechnique, EL Harrach, Algiers 16200, Algeria

ARTICLE INFO

Article history:
Received 24 January 2016
Revised 29 April 2017
Accepted 3 May 2017
Available online 4 May 2017

Keywords:
Bayesian MER detector
Cell-averaging
Order-statistics
Chi-2 targets
Interfering targets
Delay estimation

ABSTRACT

This paper addresses the thresholding problem which is an important issue in detection theory. A new thresholding methodology is proposed, namely the *Minimum Error Rate* (MER), related to the minimization of the error probability instead of minimizing only the miss probability for a *Constant False Alarm Rate* (CFAR). In an adaptive detection scheme, the proposed thresholding technique is combined with *Cell Averaging* (CA) and *Order-Statistics* OS estimation methods giving birth to the (CA-MER) and (OS-MER) detectors. Their performance statistics are analyzed for both homogeneous and heterogeneous environments. Moreover, a simplified approximate threshold expression is proposed and its effect on the whole detection process is studied. Theoretical and numerical results show that the MER-based detectors operate better than the classical CFAR-based ones. In particular, the proposed method is shown to be robust w.r.t. estimation errors on the different parameters (priors). Comparative study of MER versus CFAR-based detectors used for the delay detection in multipath context show that OS-MER detector outperforms the OS-CFAR which induces more accurate mobile positioning.

1. Introduction

Detection theory is a powerful statistical tool used for making decisions on the occurrence or non-occurrence of some event of interest. This tool has been largely used in many fields, including radar, sonar, communications, speech, image processing, biomedicine, and seismology [1,2].

The considered detection problem is a binary hypothesis testing problem of the simple hypothesis H_0 (no target is present) versus the simple hypothesis H_1 (a target is present). The most powerful tool that can be used to solve this problem is the Neyman–Pearson (NP) lemma [3,4] which maximizes the probability of detection P_d under the constraint of a constant (fixed) probability of false alarm P_{fa}. The optimal solution to the NP criterion is the *Likelihood Ratio Test* (LRT): $\Lambda \gtrless \eta$ where η is a fixed threshold ensuring a fixed P_{fa} and Λ is the likelihood ratio.

Originally for the NP-based detection, the background environment was assumed known, so that a fixed threshold could be used. However, a realistic radar environment is spatially and temporally variant, so that to maintain a constant P_{fa}, the threshold η has to be adaptively updated taking into account the changes that occur in the environment. This method of automatically tracking the threshold η is referred to as Constant False Alarm Rate (CFAR) detection. In this kind of adaptive thresholding techniques, a *Probability Density Function* (PDF) of the noise is assumed belonging to a set of parametric laws where the parameters are unknown and have to be estimated. Under the assumption of clean and homogeneous environment, measurements from the surrounding area are then used to estimate the unknown parameters on which an appropriate threshold is obtained. The simplest adaptive detector is the Cell-Averaged Constant False Alarm Rate (CA-CFAR) detector first investigated by Finn and Johnson in 1968 [5,6].

The CA-CFAR is asymptotically equivalent to a *Generalized Likelihood Ratio Test* (GLRT) where the unknown parameters are estimated using the Maximum Likelihood (ML) approach. In general, the comparison of the likelihood ratio Λ to a constant threshold η reduces to the comparison of a *Sufficient Statistic* $\mathcal{S}$ to another constant threshold γ. Using only the statistic $\mathcal{S}$ for making a decision leads to very simple decision scheme that made the success of the CA-CFAR detector and its wide range of applications, e.g. [7,8]. However, this simplicity is achieved at the expense of the optimality. In fact, the CFAR-based detectors exhibit some losses in target sensitivity as compared to the sensitivity of the optimal NP-based detectors.

As mentioned earlier, the CFAR-based detectors maximize the detection probability while keeping under control the probability of false alarm. This kind of constraint, although suitable for certain applications like radar detection and biomedical hypothesis testing, can lead to an inappropriate solution for detection problem where

* Corresponding author.
E-mail address: boudjwahab@gmail.com (A. Boudjellal).

http://dx.doi.org/10.1016/j.sigpro.2017.05.003
0165-1684/

the two detection errors have to be under control. Moreover, in some detection problems, we have prior knowledge about the signals to be detected which is not considered in the NP criterion.

The question now is how to find a new general decision approach that takes into account the two detection errors as well as the eventual prior knowledge while keeping the scheme simplicity and efficiency of the CFAR.

In this paper, we introduce a new class of adaptive detectors based on the Bayes decision rule while using the same scheme as in the CFAR-based ones. In contrast to the above mentioned approaches, this new methodology, referred to as *Minimum Error Rate* (MER), is based on the closed-form minimization of the error probability. The main difference between the MER and the CFAR resides in the process by means of which the threshold γ is selected. In contrast to the Neyman–Pearson criterion, the threshold γ is selected such that the detection error probability is minimal. Moreover, an appropriate explicit form of γ is given based on the Bayesian criterion.

Like the CFAR-based detectors, MER-based methods can be used with different estimators of the background noise power giving birth to plethora of variants that can be used in different situations and environments.

This new methodology has been used for the time-delay estimation for mobile localization in the context of multipath communications systems. Two variants have been proposed for the detection of the first arriving signal; the *Cell-Averaging Minimum Error Rate* (CA-MER) which is efficient if only one finger is present within the reference window or if the power of the first peak is high enough to shadow the other ones [11], and the *Order-Statistics Minimum Error Rate* (OS-MER) more appropriate for situations where several closely spaced paths are present within the reference window [12]. Part of this work has been presented in [11] and [12] where the optimization of the probability of error has been done numerically. Herein, we consider the general case of integrated signals and an approximate threshold γ that minimizes the error probability is given in a closed-form.

The main contributions of this paper are: (i) the introduction of a new thresholding methodology with derivation of an analytical approximate threshold value that prevents the use of fastidious numerical optimization resolution; (ii) the analysis of the gap between these two thresholds for both CA and OS-based noise power estimation; (iii) the derivation of the detection and false alarm probabilities of the CA-MER detector for the homogeneous case; (iv) the derivation of the detection and false alarm probabilities of the OS-MER detector for the homogeneous case; (v) the derivation of the detection and false alarm probabilities of the OS-MER detector for the heterogeneous case; and (vi) the application to the mobile localization and illustration of the performance gain in this context.

The remaining of this paper is organized as follows: in Section 2, we introduce the statistical formulation of the detection problem. Section 3 introduces the proposed adaptive detection scheme. In Section 4, we provide the distributions of the detection statistics that are used later for the performance analysis. Section 5 is dedicated to some comments and discussions on the proposed MER detector. In Sections 6, we study the performance of the CA-MER and OS-MER detectors, respectively. The application of the MER detector to the mobile localization problem is introduced in Section 7. In Section 8, the performance of the two detectors are assessed and discussed through extensive numerical experiments.

2. Statistical formulation of the detection problem

We consider n measurements (samples) $\{x_t\}_{t=1:n}$ of the signal under investigation. Based on these observations $\mathbf{x} = [x_1, x_2, \ldots x_n]$, we are interested in determining whether a received digital signal x_t contains a signal s_t embedded in random background noise w_t or, on the contrary, x_t is just a confusing manifestation of the noise.

$$\mathcal{T}: \begin{cases} H_0: & x_t = w_t \\ H_1: & x_t = s_t + w_t \end{cases} \Leftrightarrow \begin{cases} H_0: & \sigma_x^2 = \sigma_w^2 \\ H_1: & \sigma_x^2 = \sigma_w^2(1+S) \end{cases} \tag{1}$$

where s_t, w_t, and x_t are *i.i.d.* Gaussian and circular complex-valued random processes such that $s_t \sim \mathcal{N}(0, 2\sigma_s^2)$, $w_t \sim \mathcal{N}(0, 2\sigma_w^2)$, and $x_t \sim \mathcal{N}(0, 2\sigma_x^2)$ with $\sigma_x^2 = \sigma_w^2(1+S)$ and $S = \sigma_s^2/\sigma_w^2$ being the signal-to-noise ratio. We assume that the signal samples s_t are independent from the noise ones w_t.

One way to solve this statistical hypotheses test is to use the classical approach pioneered by Neyman and Pearson which maximizes the test power $\beta_\theta(\mathcal{T}) = P(\text{reject } H_0|H_1 \text{ is true})$ while keeping the test level $\alpha_\theta(\mathcal{T}) = P(\text{reject } H_0|H_0 \text{ is true})$[1] fixed at a low constant value α, i.e.,

$$\text{Maximize} \quad P(\text{reject } H_0|H_1) \quad s.t. \quad P(\text{reject } H_0|H_0) \leq \alpha \tag{2}$$

where $P(A)$ stands for the probability of the event A and θ is, in this case, the unknown signal and noise variances.

Using the Neyman–Pearson lemma leads to an LRT-equivalent test based on the comparison of the sufficient statistic $\mathcal{S}(\mathbf{x}) = \sum_{t=1}^{n} |x_t|^2$ to a fixed threshold γ chosen to satisfy a constraint on the test level:

$$\Lambda_{LRT}(\mathbf{x}) = \frac{f(\mathbf{x}; H_1)}{f(\mathbf{x}; H_0)} \gtrless \eta \Longleftrightarrow \mathcal{S}(\mathbf{x}) \gtrless \gamma = T\sigma_w^2 \tag{3}$$

where T is a scaling factor. The Neyman–Pearson-based detector is the optimal[2] one over all α-level tests and is referred to as a *clairvoyant* detector and can serve as a reference upper bound to which the performance of other sub-optimal detectors are compared.

When the distribution parameters of the observation are unknown, the Neyman–Pearson criterion gives rise to another sub-optimal detector. The unknown parameters are estimated and injected in the LRT giving birth to a new test referred to as the *Generalized Likelihood Ratio Test* (GLRT):

$$\Lambda_{GLRT}(\mathbf{x}) = \frac{f(\mathbf{x}; \widehat{\sigma_x}, H_1)}{f(\mathbf{x}; \widehat{\sigma_w}, H_0)} \gtrless \eta \Longleftrightarrow \mathcal{S}(\mathbf{x}) \gtrless \gamma = TZ \tag{4}$$

The test statistic $\mathcal{S}(\mathbf{x})$ is compared with the adaptive threshold γ which is the product of the noise power estimate $Z = \widehat{\sigma_w^2}$ and the scaling factor T. The method used for estimating the noise power and calculating the scaling factor defines the detector scheme and performance.

3. Adaptive detection scheme

The variable and non-stationary nature of the background environment makes the estimation of the unknown distribution parameters a challenging task. An automatic process for adaptive tracking of the unknown parameters, and hence of the detection threshold, needed to keep the GLRT-level at a constant value has been previously introduced. The adaptive detector in Fig. 1 is an implementation of the statistical test in (4). The in-phase and quadrature components of the received signal x_t are processed by a square-law detector and, eventually, an integrator. The resulting signals are set serially in a shift register referred to as the analyzing window.

The noise power is estimated using the measurements within the reference window composed of m *Reference Cells* under the assumption that the noise power is invariant over the reference cells

[1] In detection theory, the test power $\beta_\theta(\mathcal{T})$ and the test level $\alpha_\theta(\mathcal{T})$ are referred to as the probability of detection P_d and the probability of false alarm P_{fa}, respectively.

[2] It is the *Uniformly Most Powerful* one for any SNR value [3,13].

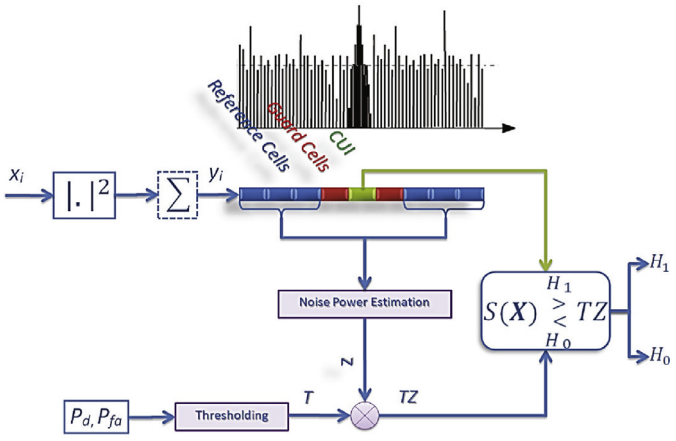

Fig. 1. Adaptive detection scheme commonly used in Radar.

time period (local stationarity assumption). The *Guard Cells*, immediate neighbors of the *Cell Under Investigation* (CUI), are excluded from the estimation process to avoid an eventual spillover from the CUI. The scaling factor T is obtained via an optimization process where the criterion is function of the probabilities of the two erroneous decisions the miss probability $P_m = 1 - P_d$ (P_d being the detection probability) and the false alarm probability P_{fa}, defined as:

$$P_{fa} = \int_0^{+\infty} f_Z(z)\left(\int_{Tz}^{+\infty} f_{\mathcal{S}|H_0}(s|H_0)ds\right)dz$$
$$P_d = \int_0^{+\infty} f_Z(z)\left(\int_{Tz}^{+\infty} f_{\mathcal{S}|H_1}(s|H_1)ds\right)dz \quad (5)$$

This adaptive thresholding process described above is known as the CFAR-based detection technique, a process by means of which a continuously changed threshold is used maintaining a constant P_{fa}. Thus, for a fixed and completely controlled P_{fa}, the first type of detection errors, the second type of detection errors, the P_m, is minimized at the best.

This way of thinking is well adapted for radar or sonar applications where a false alarm, in general, costs more than a miss event. Nevertheless, in other type of detection applications, this is not true, and both error types have to be taken into account when optimizing the detection process. For example, localization techniques based on propagation time delay, when detecting the first peak of the correlation function between the received signal and the transmitted pilot sequence, a false alarm or a miss of detection are equally harmful and both lead to localization errors.

We propose in this paper, based on the Bayes criterion, another optimization approach for an adaptive detection scheme that takes into account the two types of errors, false alarm and miss of detection, and takes advantage from the prior knowledge about the two considered hypothesis. The proposed cost function is the error probability P_e:

$$P_e = P_{H_0}P_{fa} + P_{H_1}P_m = \lambda P_{fa} + (1-\lambda)(1-P_d) \quad (6)$$

where $P_{H_0} = \lambda$ and $P_{H_1} = 1 - \lambda$ represent prior probabilities of absence and presence of a signal of interest, respectively. The optimal scaling factor is:

$$T_{MER} = argmin\ (P_e) \quad (7)$$

The analytical expression of P_e is derived in Section 6. The obtained scaling factor depends on the prior knowledge λ and is highly influenced by the method by which noise power is estimated. It is clear that (6) is a non linear and very complex function especially when the background environment is heterogeneous, the signals to be detected are fluctuating and a process of non-coherent integration is used. A closed-form solution for such a function is not easy to find and numerical methods can not ensure accurate solution because of the sensitivity of this function that can take values very close to zero. The second challenging problem is how to combine MER optimization method with the classical CFAR variants without loosing the strong aspects that makes the celebrity of CFAR-based detectors for radar detection problems, i.e., the simplicity of the detection's statistic and scheme.

4. Distributions of the detection statistics

Before proceeding to the analysis of the proposed thresholding technique and the computation of its performance, it is worthwhile to summarize some statistics that will be used for this purpose. If a Swerling-I model [14] is assumed for both primary and interfering signals, and if the noise is Gaussian, then the square law detector outputs are governed by an exponential distribution [14,15]. In general, n signal samples are incoherently-integrated before setting them to the serial shift register in the aim of improving their signal-to-noise ratio. It follows that the CUI content $\mathcal{S}$ is a Chi-square random variable with $2n$ degrees of freedom ($\mathcal{S} \sim \xi\ \chi^2_{2n}$):

$$f_{\mathcal{S}|H_j}(s|H_j) = \frac{s^{n-1}\ e^{-s/\xi}}{(\xi)^n\ \Gamma(n)}; s > 0 \quad (8)$$

$$\text{with: } \xi = \begin{cases} 2\sigma_w^2 & H_0: \text{ noise alone} \\ 2\sigma_w^2(1+S) & H_1: \text{ noise + signal} \end{cases} \quad (9)$$

Also the reference cell contents $Y_i, i = 1:m$ are Chi-square distributed random variables with $2n$ degrees of freedom:

$$Y_1, \ldots, Y_m \overset{i.i.d.}{\sim} 2\sigma_w^2\ \chi^2_{2n} \quad (10)$$

If r interfering signals are present within the reference window, the r samples U_i are Chi-square random variables with $2n$ degrees of freedom:

$$U_1, \ldots, U_r \overset{i.i.d.}{\sim} 2\sigma_w^2(1+I)\ \chi^2_{2n} \quad (11)$$

where $I = \sigma_r^2/\sigma_w^2$ is the interference-to-noise ratio and σ_r^2 is the power of the interfering signals.[3] Next, two different methods for adaptive noise power estimation by processing the reference cell contents are presented.

4.1. Distribution of the cell-averaging output

The *Cell-Averaging* (CA) process is the ML-based estimation of the noise power estimate $Z = \sum_{i=1}^{m} Y_i$. Under the assumption of homogeneous environment, Z is Chi-square distributed with $2nm$ degrees of freedom:

$$Z \sim 2\sigma_w^2\ \chi^2_{2nm} \quad (12)$$

In presence of r interfering signals within the reference cells, the $m-r$ noise samples Y_i and the r interfering samples U_i are Chi-square random variables with $2n$ degrees of freedom:

$$\begin{array}{lll} Y_i \overset{i.i.d.}{\sim} & 2\sigma_w^2\ \chi^2_{2n}, & i = 1, 2, \ldots, m-r \\ U_j \overset{i.i.d.}{\sim} & 2\sigma_w^2(1+I)\ \chi^2_{2n}, & j = 1, 2, \ldots, r \end{array} \quad (13)$$

Hence, the noise power estimate is the sum of two independent random variables not equally distributed Y and U:

$$\begin{array}{lll} Y = \sum_{i=1}^{m-r} Y_i & \Rightarrow & Y \sim 2\sigma_w^2\ \chi^2_{2n(m-r)} \\ U = \sum_{i=1}^{r} U_i & \Rightarrow & U \sim 2\sigma_w^2(1+I)\ \chi^2_{2nr} \end{array} \quad (14)$$

The PDF of Z is a function of those of U and Y and can be computed as the convolution of the two distributions:

$$f_Z(z) = \int f_U(z-y) f_Y(y) dy \quad (15)$$

[3] We consider herein that the r interfering signals have the same power σ_r^2.

4.2. Distribution of the order-statistics output

The Order-Statistics method has been successfully used for estimating the noise power in heterogeneous environment or in presence of interfering signals, e.g. [9]. In this method, the reference cells' contents are sorted in increasing order $Y_{(1)} \leq Y_{(2)} \leq \ldots \leq Y_{(k)} \leq \ldots \leq Y_{(m)}$. Then, the noise power is estimated as the content of reference cell having the kth rank [16–19]

$$Z = Y_{(k)} \tag{16}$$

Under the assumptions of homogeneous environment, the distribution of the kth-rank sample $Y_{(k)}$ are given by [20]:

$$\begin{aligned} f_Z(z) &= kC_k^m (1-F_Y(y))^{m-k} (F_Y(y))^{k-1} f_Y(y) \\ F_Z(z) &= \sum_{j=k}^{m} C_j^m (F_Y(y))^j (1-F_Y(y))^{m-j} \end{aligned} \tag{17}$$

$f_Y(y)$ being the probability density function given by (10) and $F_Z(z)$ refers to the cumulative function of Z.

However, if r interfering signals appear in the reference window, the noise power estimate Z is chosen as the content of reference cell having the kth rank in the more general set $\{U_j\}_{j=1,2,\ldots,r} \cup \{Y_i\}_{i=1,2,\ldots,m-r}$. The probability distribution function of Z can be computed using those of the Chi-square random variables U_i and Y_i, given in (13), as follows:

$$\begin{aligned} F_Z(z) = &\sum_{i=k}^{m} \sum_{j=min(0,i-r)}^{max(i,m-r)} C_j^{m-r} C_{i-j}^r (F_Y(y))^j \\ &(1-F_Y(y))^{m-r-j} (F_U(u))^{i-j} (1-F_U(u))^{r-i+j} \end{aligned} \tag{18}$$

5. Discussions

We present herein some comments on the proposed detection scheme as well as a useful threshold approximation and its statistical analysis.

5.1. MER vs CFAR

A main advantage of the CFAR as compared to MER detector lies in the fact that the scaling factor for the former is easy to compute (an analytical expression exist) and depends on the P_{fa} only [13]. For the MER we need, as for the GLRT, to estimate (or a priori known) other system parameters which are λ and S. As will be shown in Section 8, when the number of samples is moderate or large, the sensitivity of the MER is robust against estimation errors on these two parameters. On the other hand, the MER outperforms the CFAR in terms of error probability in a large range of SNR values depending on the sample size n and hence is more adequate for the mobile localization problem discussed next.

5.2. Approximate threshold expression

The MER-based thresholding consists of finding the optimal scaling factor T that minimizes the error probability in (6). As stated in Section 3, the complex formulas of P_d and P_{fa} and the numerical sensitivity of the error function P_e makes the minimization of (6) a hard optimization problem.

For this reason, we introduce herein an approximate analytical expression of the scaling factor T. Indeed, the derivation of the MER-based detector can be seen as a special case of the more general Bayesian detector given by the *Conditional Likelihood Ratio Test* (CLRT) [1,10]:

$$\Lambda_{CLRT}(\mathbf{x}) = \frac{f(\mathbf{x}|H_1)}{f(\mathbf{x}|H_0)} \gtrless \eta = \frac{P_{H_0}}{P_{H_1}} \quad \Leftrightarrow \mathcal{S}(\mathbf{x}) \gtrless \gamma = T\sigma_x^2 \tag{19}$$

where $\mathcal{S}(\mathbf{x})$ is the sufficient statistic and T is the scaling factor that minimizes the error probability in (6) and given by[4]:

$$T = \log\left[\left((1+S)^n \ \eta \right)^{\frac{1+S}{S}} \right] \tag{20}$$

In a case, the noise power σ_w^2 is replaced by its estimate Z leading to:

$$\gamma = TZ = \overline{T}\sigma_w^2 \tag{21}$$

where $\overline{T} = T\frac{Z}{\sigma_w^2}$. Thus, in this case, the scaling factor that minimizes (6) is a random variable. If Z is a consistent estimator of the noise power, then the scaling factor T in (20) will be a good approximation of $\overline{T}$. The behavior of this estimate is analyzed numerically in Section 8. Below, we provide a theoretical analysis of the first and second order statistics of $\overline{T}$.

5.3. Statistical analysis of $\overline{T}$

The aim of this subsection is to compute a confidence interval for $\overline{T}$ and see if the approximate threshold T is included inside it. For the CA-MER detection, the noise power is estimated as the mean of $2nm$ Gaussian samples $x_t, t = 1:2nm$. It follows that $Z = \widehat{\sigma_w^2}$ is Chi-square distributed with $2nm$ degrees of freedom $Z \sim \frac{\sigma_w^2}{2nm}\ \chi^2_{2nm}$. Hence, $\overline{T} = T\frac{Z}{\sigma_w^2}$ is also Chi-square distributed with $2nm$ degrees of freedom $\overline{T} \sim \frac{T}{2nm}\ \chi^2_{2nm}$ such that $\mu_{\overline{T}} = T$ and $\sigma^2_{\overline{T}} = \frac{T^2}{nm} \underset{nm\to\infty}{\longrightarrow} 0$.

Once the statistical distribution of scaling factor $\overline{T}$ is completely defined, we can infer the following exact confidence interval I_α^1 of level $\alpha = \alpha_1 + \alpha_2$:

$$\overline{T} \in I_\alpha^1 = \left[T\frac{Q_{\chi^2_{2nm},\alpha_1}}{2nm},\ T\frac{Q_{\chi^2_{2nm},1-\alpha_2}}{2nm} \right] \tag{22}$$

such that $P(\overline{T} \in I_\alpha^1) = 1-\alpha$. The quantities $Q_{\chi^2_{nm},\alpha_1}$ and $Q_{\chi^2_{nm},1-\alpha_2}$ are the quantiles of the Chi-square distribution of level α_1 and $1-\alpha_2$, respectively. In our simulation experiments (Fig. 4), one uses (22) with $\alpha_1 = \alpha_2 = 0.025$.

5.4. Analysis of the noise power estimate in OS-MER

The noise power is evaluated in OS-MER case as the kth order statistic, thus, as we will see, Z is a biased estimation of σ_w^2. Below we evaluate the bias of this estimate in both homogeneous and heterogeneous environment cases. Under the statistical model in (13), the mean value of Z (given by (16), in the heterogeneous case, is equal to:

$$\begin{aligned} E[Z] = 2\sigma_w^2 &\sum_{i=k}^{m} \sum_{j=max(0,i-r)}^{min(i,m-r)} C_j^{m-r} C_{i-j}^r \sum_{p=0}^{j} \sum_{q=0}^{i-j} C_p^j C_q^{i-j} (-1)^{i-p-q} \sum_{|\vec{i}|=m-r-p} \\ &\frac{C^{m-r-p}_{i_1,\ldots,i_{n-1}}}{\prod_{t=0}^{n-1}(t!)^{i_t}} \sum_{|\vec{j}|=r-q} \frac{C^{r-q}_{j_0,\ldots,j_{n-1}}}{\prod_{t=0}^{n-1}(t!)^{j_t}} \frac{\left(\frac{1}{1+I}\right)^{\sum_{t=0}^{n-1} t j_t} \Gamma\left(\sum_{t=0}^{n-1}(i_t+j_t)t+1\right)}{\left(m-r-p+\frac{r-q}{1+I}\right)^{\sum_{t=0}^{n-1}(i_t+j_t)t+1}} \end{aligned} \tag{23}$$

and in the homogeneous case (under the statistical model in (17)), the mean value of Z is given by:

$$E[Z] = 2\sigma_w^2 \frac{kC_k^m}{\Gamma(n)} \sum_{i=0}^{k-1} C_i^{k-1} (-1)^{k-i-1}$$

[4] The derivation of (20) comes from (19) and the Gaussian assumption i.e. $x_t \overset{H_1}{\sim} \mathcal{N}(0, 2\sigma_x^2)$ and $x_t \overset{H_0}{\sim} \mathcal{N}(0, 2\sigma_w^2)$.

$$\times \sum_{\left|\vec{j}\right|=m-1-i} \frac{C_{j_0,\ldots,j_{n-1}}^{m-1-i}}{\prod_{t=0}^{n-1}(t!)^{j_t}} \frac{\Gamma\left(\sum_{t=0}^{n-1} t j_t + n + 1\right)}{(m-i)^{\left(\sum_{t=0}^{n-1} t j_t + n + 1\right)}} \tag{24}$$

where $\vec{j} = (j_0, \ldots, j_{n-1})$, $|\vec{j}| = \sum_{t=0}^{n-1} j_t$ and $C_{j_0,\ldots,j_{n-1}}^{m-1-i}$ are the multinomial coefficients. Clearly this is of the form $E[Z] = C\ \sigma_w^2$ where C depends on k (the statistic order) and I (the interference to noise ratio). In the homogeneous case, C depends on k only and hence the estimator bias can be 'corrected' which reduces the performance loss (as compared to CA-CFAR in the homogeneous case). This issue will be the focus of future work.

6. Performance analysis

In this section, we assess the performance of the adaptive MER detector presented in Fig. 1 which is an implementation of the hypothesis test given in (3). By detector performance we mean the detection and false alarm probabilities needed for the derivation of the optimal scaling factor T.

6.1. Performance analysis of CA-MER detector

For an homogeneous environment, the pdf of Z is given in (12) and the detection probability is expressed by [15]:

$$P_d = (1+V)^{-mn} \sum_{i=0}^{n-1} \frac{1}{i!} \frac{\Gamma(mn+i)}{\Gamma(mn)} \left(\frac{V}{1+V}\right)^i \tag{25}$$

with $V = \frac{T}{1+S}$, and $\Gamma(.)$ is the gamma function.

6.2. CA-MER losses in heterogeneous environment

When the assumption of homogeneous background environment is no longer respected, the performance of the MER detector degrades in a drastically manner. If in addition to the primary signal, r i.i.d interfering signals are then present in the reference cells, the pdf of Z is given by (14) and (15) and the probability of detection is given by the following theorem.

Theorem 1. *Under the assumptions presented in (14) for the heterogeneous model, the detection probability of the test presented in (3), when using the cell averaging for the noise power estimate, is given by:*

$$\begin{aligned} P_d = {} & \frac{(1+I)^{-rn}\left(\frac{I}{1+I}\right)^{-mn}}{\Gamma(rn)\Gamma(mn-rn)} \sum_{i=0}^{rn-1} C_i^{rn-1}(-1)^i \Gamma(mn-rn+i) \\ & \left\{ \left(\frac{I}{1+T\frac{1+I}{1+S}}\right)^{rn-i} \sum_{l=0}^{n} \frac{\Gamma(rn-i+l)}{l!} \left(\frac{\frac{T}{1+S}}{\frac{1}{1+I}+\frac{T}{1+S}}\right)^l \right. \\ & - \left(\frac{\frac{I}{1+I}}{1+\frac{T}{1+S}}\right)^{rn-i} \sum_{j=0}^{mn-rn+i-1} \frac{1}{j!} \left(\frac{\frac{I}{1+I}}{1+\frac{T}{1+S}}\right)^j \\ & \left. \times \sum_{l=0}^{n} \frac{\Gamma(rn-i+j+l)}{l!} \left(\frac{\frac{T}{1+S}}{1+\frac{T}{1+S}}\right)^l \right\} \end{aligned} \tag{26}$$

Proof. The proof is given in Appendix A. □

The probabilities of false alarm P_{fa} are obtained by setting $S = 0$ in the Eqs. (25) and (26).

6.3. Performance analysis of OS-MER detector

The CA-CFAR and CA-MER are efficient approaches when the background environment is homogeneous. However, if some outliers take place within the m noise samples, the averaging of the latter leads to biased estimation of the noise power which affects drastically the whole detection process. To cope with this problem, a robust CFAR-based detector, namely the *Order-Statistics Constant False Alarm Rate* (OS-CFAR), has been introduced in [16]. The reference cell outputs are sorted in increasing order and the noise power is adaptively estimated as the content of reference cell having the kth rank. For the OS-MER, the same estimate of the noise power is used leading to the following detection probability in the homogeneous environment.

Theorem 2. *Under the assumptions given in (17) for homogeneous model, the detection probability of the test presented in (3), when using the kth order statistic for the noise power estimate, is given by:*

$$\begin{aligned} P_d = {} & \frac{kC_k^m}{\Gamma(n)} \sum_{i=0}^{k-1} C_i^{k-1}(-1)^{k-i-1} \sum_{\left|\vec{j}\right|=m-1-i} \frac{C_{j_0,\ldots,j_{n-1}}^{m-1-i}}{\prod_{t=0}^{n-1}(t!)^{j_t}} \\ & \times \sum_{l=0}^{n-1} \left(\frac{T}{1+S}\right)^l \frac{\Gamma\left(\sum_{t=0}^{n-1} t j_t + n + l\right)}{l!\left(m-i+\frac{T}{1+S}\right)^{\sum_{t=0}^{n-1} t j_t + n + l}} \end{aligned} \tag{27}$$

Proof. The proof is given in Appendix B. □

6.4. OS-MER losses in heterogeneous environment

In this subsection, our aim is to quantify the performance degradation of the OS-MER detector caused by the presence of r interfering signals. In this context, the probability of detection is given by the following theorem.

Theorem 3. *Under the assumptions given in (18) for the heterogeneous model, the detection probability of the test presented in (3), when using the kth order statistic for the noise power estimate, is given by:*

$$\begin{aligned} P_d = {} & \frac{\left(\frac{T}{1+S}\right)^n}{\Gamma(n)} \sum_{i=k}^{m} \sum_{j=max(0,i-r)}^{min(i,m-r)} C_j^{m-r} C_{i-j}^{r} \sum_{p=0}^{j} \sum_{q=0}^{i-j} C_p^j C_q^{i-j} (-1)^{i-p-q} \sum_{\left|\vec{p}\right|=m-r-p} \\ & \frac{C_{p_0,\ldots,p_{n-1}}^{m-r-p}}{\prod_{t=0}^{n-1}(t!)^{p_t}} \sum_{\left|\vec{q}\right|=r-q} \frac{C_{q_0,\ldots,q_{n-1}}^{r-q}}{\prod_{t=0}^{n-1}(t!)^{q_t}} \frac{\left(\frac{1}{1+I}\right)^{\sum_{t=0}^{n-1} t q_t} \Gamma\left(\sum_{t=0}^{n-1}(p_t+q_t)t+n\right)}{\left(m-r-p+\frac{T}{1+S}+\frac{r-q}{1+I}\right)^{\sum_{t=0}^{n-1}(p_t+q_t)t+n}} \end{aligned} \tag{28}$$

Proof. The proof is given in Appendix C. □

7. Application to mobile positioning

We consider herein the application of the MER concept to the detection of the first channel path for mobile positioning in the context of multipath communications system.

7.1. Multipath channel model

In mobile communications, the specular *Channel Impulse Response* (CIR) is often modeled as a noisy version of a time-varying linear filter [21,22]:

$$h(t) = \left\{ \sum_{j=1}^{R} \alpha_j(t)\ \delta(t-\tau_j(t)) \right\} + w(t) \tag{29}$$

where $\tau_j(t)$ and $\alpha_j(t)$ are the time-varying delay and the time-varying complex amplitude of the jth path, respectively, R is the number of the signal copies at the receiver end, and $w(t)$ is a zero-mean Gaussian complex-valued noise with variance $2\sigma_w^2$. It is usual to assume that paths' complex amplitudes remain constant over a slot (packet) duration and are modeled as *i.i.d* slot-varying Gaussian random complex-valued processes. Time delays are usually assumed constant over several slots (n slots) [23]. Taking into

account these two assumptions, the shaping filter effect, and assuming that the CIR vanishes outside an interval [0, M], where M represents the channel length,[5] the CIR over the slot l will be [24]:

$$h_l(i) = \left\{ \sum_{j=1}^{R} \alpha_{j,l}\, g(iT_s - \tau_j) \right\} + w_l(i), \quad i = 0, 1, \ldots, M \tag{30}$$

where iT_s is the sampled version of t and $g(.)$ denotes the shaping filter. Note that index l has been added to refer to the slot-dependency of the considered channel parameters.

7.2. Time of arrival estimation

In a multipath context, the *Time of Arrival Estimation* (ToA) is estimated as the location of the first peak of the *Power Delay Profile* (PDP)-like function defined as the mean of the CIR over n slots: $P_i = \sum_{l=1}^{n} |h_l(i)|^2, i = 0, 1, \ldots, M$ Our objective now is to detect the first peak of the PDP-like function P_i and estimate its corresponding delay τ_1. Peak detection requires the use of a threshold γ to detect only peaks corresponding to effective channel fingers.

7.3. Detection scheme and stochastic assumptions

We assume that the first finger of the communications channel is our primary target. The other fingers are considered as interfering targets, and all of them are buried in a homogeneous background noise. For the path detection, we consider the detection scheme in Fig. 1 with $m < M$ reference cells in the vicinity of the CUI. We assume that the observation in the CUI is independent from the m outputs of the reference cells. The latter are mutually independent but are not identically distributed if some of their outputs are considered as interfering peaks.

Channel fading coefficients $\alpha_{j,l}$ for $j \neq 1$ are slot-varying Gaussian variables of variance[6] $2\sigma_w^2(1+I)$ and their corresponding delays τ_j are constant over an observation period of n slots. Under these assumptions, the PDP-like samples $P_i, i = 0, 1, \ldots, M$ are Chi-square distributed random variables with $2n$ degrees of freedom $P_i \sim \xi\, \chi^2_{2n}$ according to one of the following three situations[7]: (i) for the CUI the value of ξ is:

$$\xi = \begin{cases} 2\sigma_w^2 & H_0: \text{ noise alone} \\ 2\sigma_w^2(1+S) & H_1: \text{ noise + first peak} \end{cases} \tag{31}$$

where $S = \sigma_1^2/\sigma_w^2$ is the signal-to-noise ratio of the first peak.

(ii) for the m reference cells $\xi = 2\sigma_w^2$, (iii) if one or more interfering peaks appear in the reference cells, the m observations are statistically independent, but are no more identically distributed. In this case, for the reference cells which contain an interfering peak, $\xi = 2\sigma_w^2(1+I)$.

Under the above assumptions, the considered problem is similar to the one theoretically analyzed in the previous sections and hence the developed theory can be used to solve it. Section 8 present some results of applying the MER detection method for the estimation of the signal delay. Once the signal delays are estimated w.r.t. different base stations (at least three), one estimates the mobile position using the trilateration technique [25].

[5] In practical situations, the channel is estimated by correlating pilot signal with received signal in which case M would represent the length of estimated correlation sequence.

[6] We assumed here that all interfering paths have equal powers.

[7] For simplicity, we do not take into account the shaping filter g (in practice the latter is known ant its effect can be mitigated).

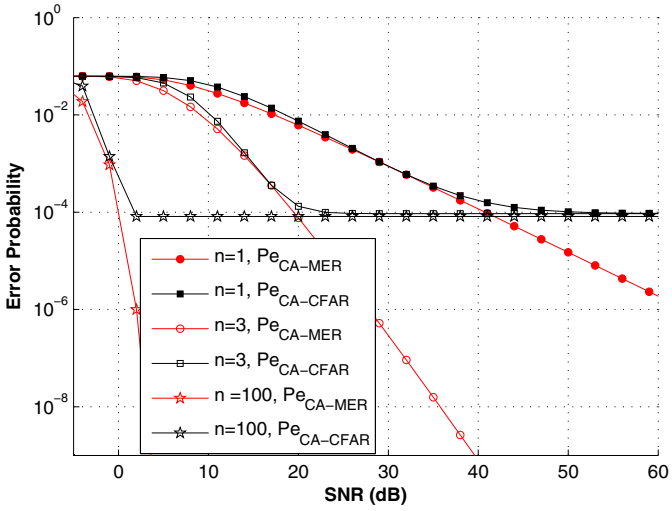

Fig. 2. CA-MER vs CA-CFAR: Error probability vs SNR.

8. Numerical results

Some numerical results are presented in this section in order to assess the performance of the adaptive MER detector. Basically, two scenarios will be conducted, one for each used estimation method i.e. CA and OS. For these two scenarios, performance of MER-based detectors are compared to those of CFAR-based ones. In all the following simulations, unless specified otherwise, the size of the reference cells m is set to 15, the pre-fixed probability of false alarm of the CFAR-based detectors is set to 10^{-4}, and the number of interfering signals within the reference window r is set to 0.

These simulation experiments are divided in four different parts dedicated to the performance assessment of CA-MER, the performance assessment of OS-MER, an analysis of the scaling factor sensitiveness w.r.t. different system parameters and to the mobile localization application, respectively.

8.1. CA-MER performance assessment

Fig. 2 depicts the behavior of the probability of error vs SNR. One can see that the error probability of the CA-MER is less than that of the CA-CFAR for all SNR values. The gap between the two curves becomes significant for high SNR values (SNR> 50 dB). The reason of this is that the error probability of the CA-CFAR detector is dominated by the a priori fixed probability of false alarm for high SNR values. The same results can be obtained for relatively low SNR if incoherent integration process is used which is advantageous for the CA-MER detector. Indeed, the Fig. 2 shows that we obtain similar results at 20 dB for $n = 3$ and at 0 dB for $n = 100$. Fig. 3 shows that for high SNR (SNR> 50 dB) a small loss in the detection probability of the CA-MER as compared to the CA-CFAR is noticed. However, the false alarm rate of the latter is hundreds times higher than that of the CA-MER.

The set of curves presented in Fig. 4 depicts the behavior of the optimal scaling factor T vs SNR for $n = 1$. We see that the exact scaling factor, referred to as T_{Ex}, obtained through numerical optimization of (7) is approximately within the 95% *Confidence Interval* (CI) of the approximated scaling factor given in (21), referred to as T_{Ap}. The effect of approximating the scaling factor by its theoretical formulas is presented in Fig. 5. For small SNR values, there is no noticeable difference between the probability of error computed using the approximated scaling factor and the probability of error computed using the exact scaling factor. The gap between the two curves increases as the SNR increases.

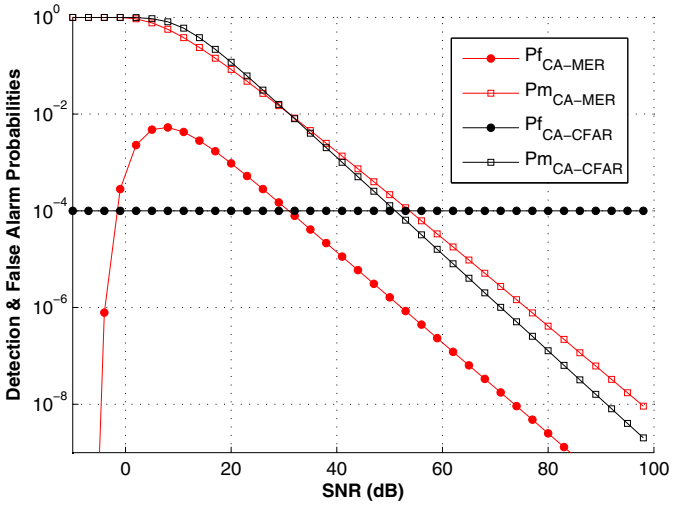

Fig. 3. CA-MER vs CA-CFAR: False alarm and miss probabilities.

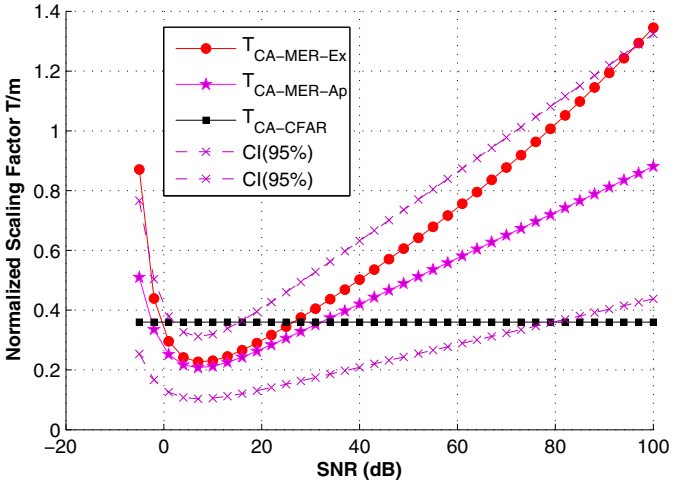

Fig. 4. CA-MER vs CA-CFAR: Scaling factor vs SNR for $n = 1$.

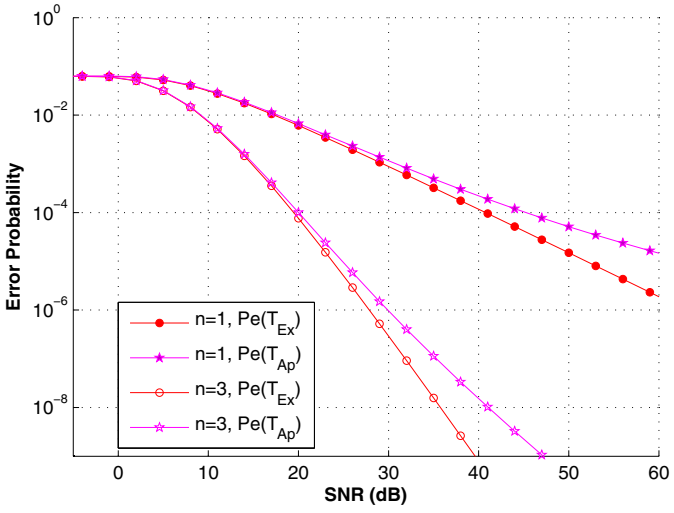

Fig. 5. CA-MER: Scaling factor approximation effect.

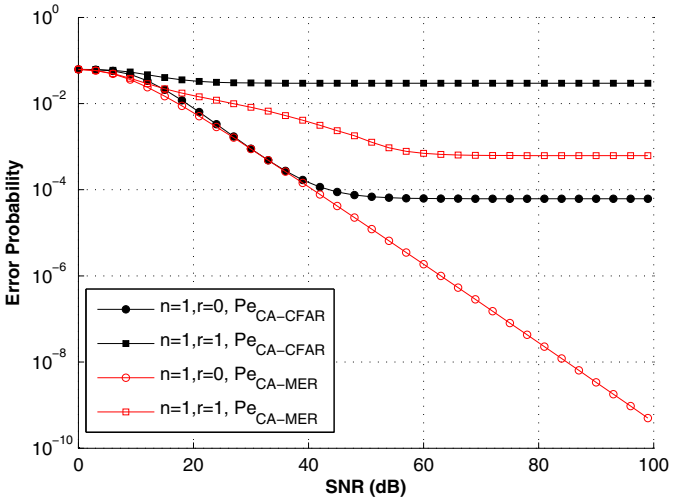

Fig. 6. CA-MER vs CA-CFAR: Interfering signals effect.

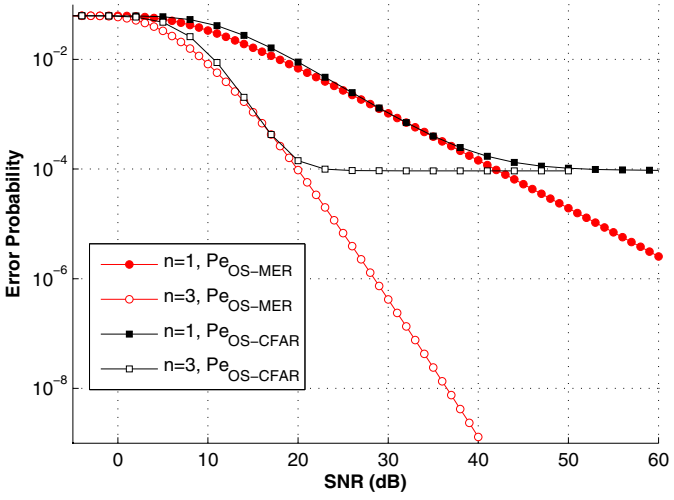

Fig. 7. OS-MER vs OS-CFAR: Error probability vs SNR.

The effect of interfering signals on the CA-MER detector is presented in Fig. 6. One can see that for only one interfering signal (i.e. $r = 1$ and $I = 20$ dB), the performance of the CA-CFAR and CA-MER detectors present serious degradation with small advantage in favor of the latter detector.

8.2. OS-MER performance assessment

In the second set of numerical experiments, the order-statistics are combined with the MER thresholding technique giving birth to the OS-MER detector which is supposed to be more robust regarding the interference effect. Unless specified otherwise, the rank of the reference cell chosen as estimate of the noise power k is set to $2m/3$.

The error probabilities of OS-CFAR and OS-MER detectors are presented in Fig. 7 for $r = 0$. Like the CA-MER detector, for high SNR values, the error probability of the OS-MER detector is very small comparatively to the error probability of the OS-CFAR detector. This result can be obtained for relatively small SNR values when n increases (e.g. 15 dB for $n = 3$).

The set of curves presented in Fig. 8 depicts the behavior of the scaling factor versus SNR. As we can see, the gap between approximated and exact threshold values increases with the SNR value and hence the effectiveness of the approximated scaling factor T_{Ap}

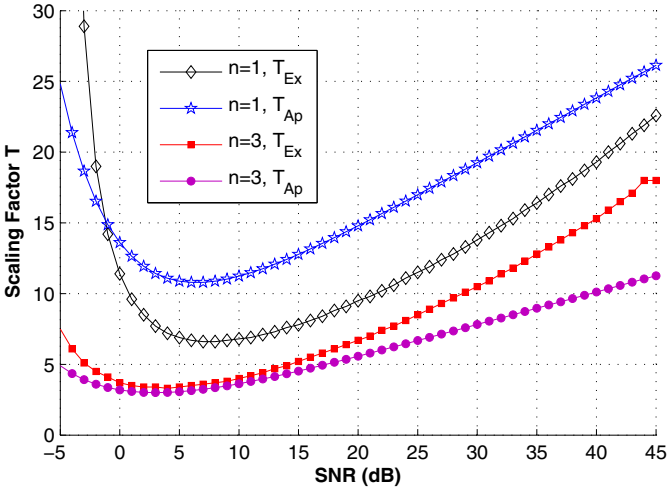

Fig. 8. OS-MER: Approximated and exact scaling factors vs SNR.

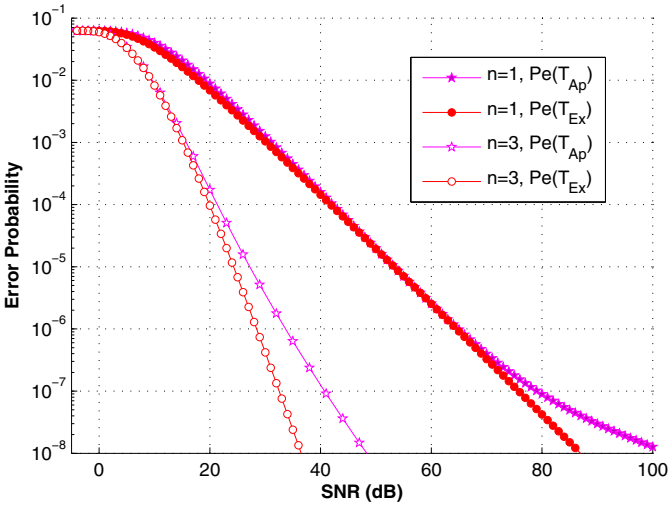

Fig. 9. OS-MER: Scaling factor approximation effect.

holds for low or medium SNRs only. Fig. 9 shows the effect of approximating the scaling factor by the formula (20). For $n = 1$, the gap between the two thresholds appears at very high SNR (SNR> 70 dB) while for $n = 3$ it starts from SNR= 20 dB.

Figs. 10 and 11 depict the effect of interfering signals on the OS-MER detector performance for $n = 1$ and $n = 2$, respectively. As one can see, the OS-MER present small performance losses for $r < 6$ interfering signals. Drastic performance losses are noticed for $r \geq 6$. Although the OS-MER present less performance degradation as compared to the OS-CFAR, this latter is robust just for a limited number of interfering signals $r \leq m - k$.

8.3. Sensitiveness analysis

In the following, we investigate the sensitiveness of the scaling factor to the estimation error on the SNR S and the prior λ. The plots in Figs. 12 and 13 illustrate the dependency of the scaling factor on the SNR for different integrated pulse number n and different reference cell number m, respectively. From these plots, one can see that the only way to reduce the sensitiveness of the scaling factor w.r.t. estimation errors on the SNR S would be to increase the reference cell size m.

In Fig. 14, we illustrate the performance loss when the thresholding factor is computed with an erroneous value of parameter S.

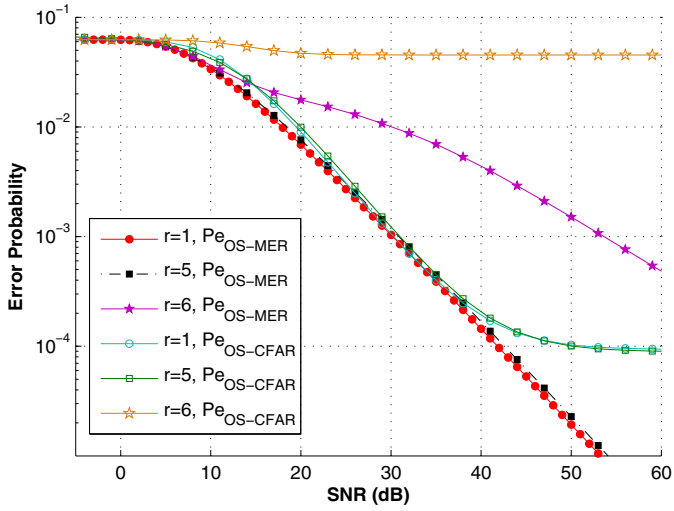

Fig. 10. OS-MER vs OS-CFAR: Interfering signals effect for $n = 1$.

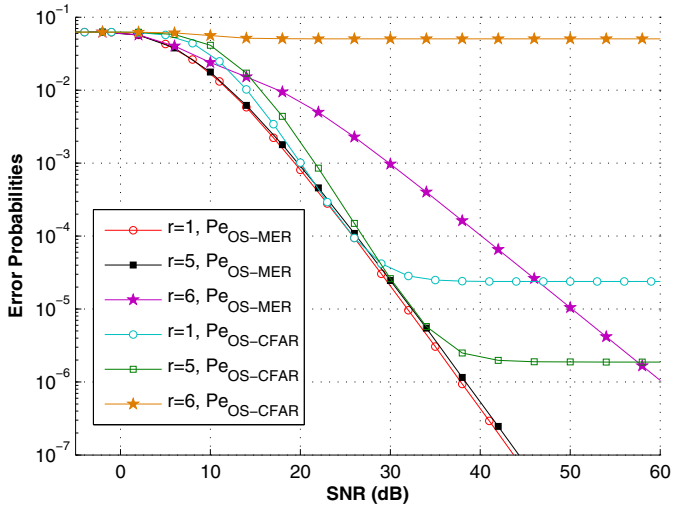

Fig. 11. OS-MER vs OS-CFAR: Interfering signals effect for $n = 2$.

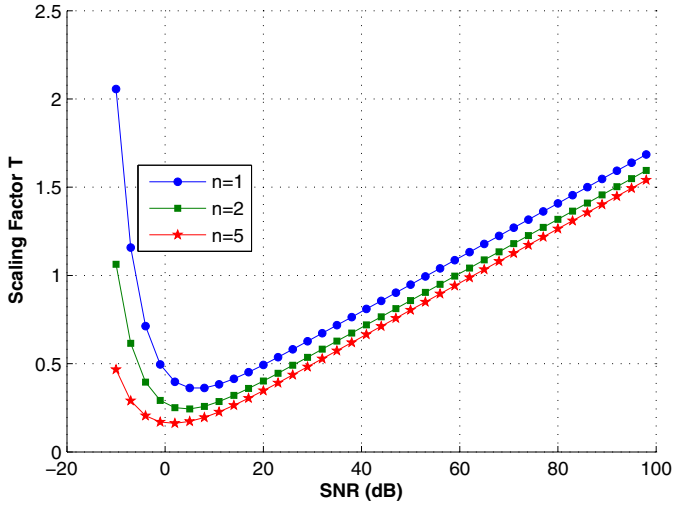

Fig. 12. Scaling Factor vs SNR for different n values.

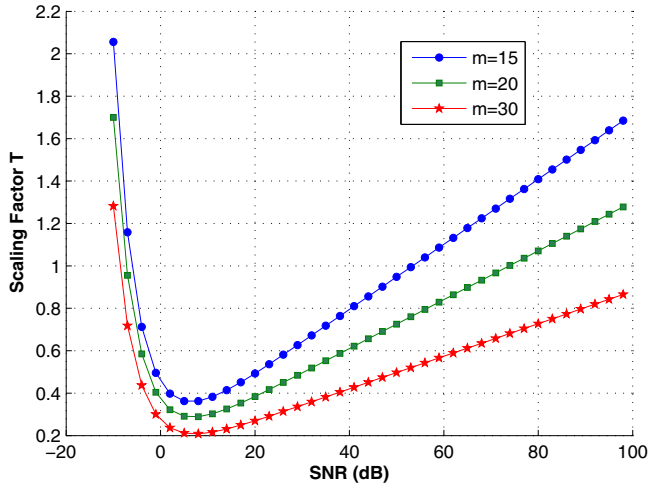

Fig. 13. Scaling Factor vs SNR for different m values.

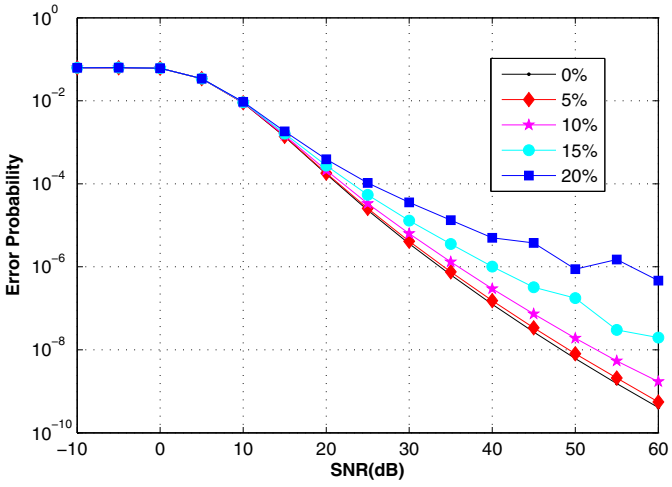

Fig. 14. Influence of SNR estimation error on P_e.

We consider the OS-MER detector for $n = 3,\ r = 0$ with different levels of SNR estimation errors corresponding to relative standard deviations equal to 5%, 10%, 15% and 20%, respectively. The performance loss is quite small for 5% or 10% estimation error levels. Even for higher estimation error levels, the performance of the OS-MER remains better than that of the OS-CFAR (which error probability is higher than 10^{-4}).

Fig. 15 illustrates the dependency between the scaling factor and the prior about the absence of a signal of interest λ for different pulse integration number n. One can see that there are strong dependency between these two parameters for the ranges $\lambda < 0.1$ and $\lambda > 0.9$ which means that small shift of λ leads to an important shift of the scaling factor. Weak dependency can be achieved by increasing the pulse integration number n. Also, the dependency is quite weak in the range $[0.1 - 0.9]$.

8.4. MER application to mobile localization

Finally, to assess the performance of the proposed OS-MER thresholding method and to compare its behavior w.r.t. OS-CFAR method when using it for delay estimation in a mobile localization context, the following numerical experiment is conducted. A Rayleigh fading channel modeling a multipath suburban outdoor environment is generated. According to [26], it consists of a B-Channel corresponding to a pedestrian mobile with speed of

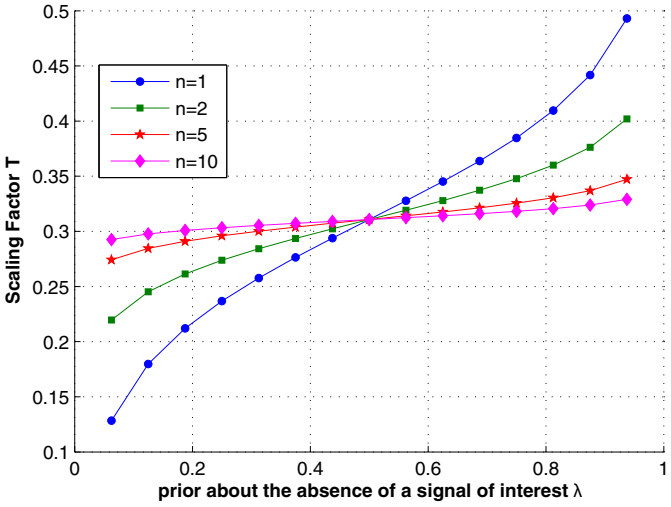

Fig. 15. Scaling Factor vs λ for different n values.

Table 1
Outdoor pedestrian B-Channel parameters [26].

Finger	1	2	3	4	5	6
Delay (nsec)	0	200	800	1200	2300	3700
Avg. Power (dB)	0	−0.9	−4.9	−8.0	−7.8	−23.9

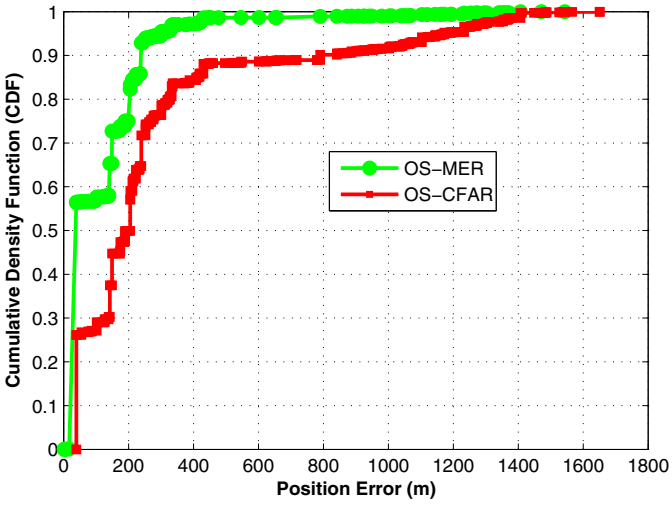

Fig. 16. OS-MER vs OS-CFAR: Cumulative Density Function.

3 km/h. The B-Channel contains six fingers and is the median spread delay case that occurs frequently (see Table 1). This generated fading channel is buried in complex-valued Gaussian noise of variance −5dB. The noisy channel coefficients are sequentially passed through an analyzing window formed of $m = 15$ reference cells surrounding the CUI. The probability of a peak value is set to $1 - \lambda = 1/m$. The slot number n is set to 3 and the statistic-order k is set to 9. The OS-CFAR and OS-MER detectors are used for delay estimation and the trilateration technique [25] is used to estimate the mobile station position, located at (400 m, 1200 m) using delay measurements relative to four base stations (BS) located at (0 m, 1325 m), (325 m, 1000 m), (325 m, 1650 m), and (650 m, 1325 m).

Fig. 16 shows the cumulative density functions (CDFs) of the location error of the detectors. One can see that for the considered scenario, the positioning algorithm based on the OS-MER detector performs better than the one based on the OS-CFAR detector.

When using the OS-MER-based detector, the positioning errors are less than 200m for 85% of the time while they are more than 300 m for the same probability using the CFAR-based detector to estimate the delay.

9. Conclusion

In this paper the thresholding step in a detection process has been explored through many theoretical results that have been assessed by numerical experiments. A new detection methodology, referred to as *Minimum Error Rate* (MER), is proposed tacking advantage from the simplicity and efficiency of the CFAR-based detectors but in contrast to the latter, the detection threshold is computed through the minimization of the error probability which is appropriate in many application fields including the mobile localization problem. The proposed MER-based detection technique has the advantage of taking into account the prior knowledge about the presence of the signal of interest. Another contribution is an approximate threshold expression easier to evaluate and suitable in many application contexts. The consistence of MER-based detection methodology is illustrated through numerical experiments in both homogeneous and heterogeneous background environment. In particular, the numerical analysis has shown a good robustness of the proposed thresholding technique w.r.t. estimation errors on parameters S and λ.

Appendix A

To evaluate the performance losses of the CA-MER detector caused by the presence of interfering signals when detecting incoherently-integrated signals we need to develop the PDF of the noise power estimate Z first. The latter can be computed, in this case, using (14) and (15). Considering the following notations $a = 2\sigma_w^2(1+S)$, $b = 2\sigma_w^2(1+I)$, $c = 2\sigma_w^2$, $d = \frac{b^{-nr}}{\Gamma(nr)}\frac{c^{-nm+nr}}{\Gamma(nm-nr)}$, the PDF of Z will be:

$$\begin{aligned} f_Z(z) &= d\ e^{-z/b}\int_0^z (z-y)^{nr-1}\ y^{nm-nr-1}\ e^{-y(I/b)}dy \\ &= d\sum_{k=0}^{nr-1} C_k^{rn-1}(-1)^k z^{nr-1-k}\ e^{-z/b}\int_0^z y^{nm-nr-1+k}\ e^{-y(I/b)}dy \\ &= d\sum_{k=0}^{nr-1} C_k^{rn-1}(-1)^k z^{nr-1-k}\ e^{-z/b}\left(\frac{I}{b}\right)^{nm-nr+k} \\ &\quad \times\gamma\left(nm-nr+k, \frac{Iz}{b}\right) \end{aligned} \tag{A.1}$$

with $\gamma(s,x) = \int_0^x t^{s-1}e^{-t}dt = \Gamma(s) - \Gamma(s,x)$ is the lower incomplete gamma function, $\Gamma(s,x) = \int_x^\infty t^{s-1}e^{-t}dt$ is the upper incomplete gamma function, and $\Gamma(s) = \int_0^\infty t^{s-1}e^{-t}dt$ is the complete gamma function. The lower incomplete gamma function in (A.1) is given by:

$$\Gamma(nm-nr+k)\left(1 - e^{-z/c}\sum_{j=0}^{nm-nr+k-1}\frac{(zI/b)^j}{j!}e^{-zI/b}\right) \tag{A.2}$$

Substituting (A.2) in (A.1) leads to:

$$\begin{aligned} f_Z(z) &= d\sum_{k=0}^{nr-1} C_k^{rn-1}(-1)^k\left(\frac{I}{b}\right)^{nm-nr+k}\Gamma(nm-nr+k) \\ &\quad \left\{ z^{nr-1-k}\ e^{-z/b} - \sum_{j=0}^{nm-nr+k-1}\frac{(I/b)^j}{j!}z^{nr-1-k+j}\ e^{-z/c}\right\} \end{aligned} \tag{A.3}$$

To calculate the detection probability defined in (5), we need to develop the following integral $I(Tz) = \int_{Tz}^{+\infty} f_{S|H_1}(s|H_1)ds$. By Replacing $f_{S|H_1}(s|H_1)$ given in (8) with $\xi = 2\sigma_w^2(1+S)$, the integral will be:

$$\begin{aligned} I(Tz) &= \int_{Tz}^{+\infty} f_{S|H_1}(s|H_1)ds = \int_{Tz}^{+\infty}\frac{s^{n-1}\ e^{-s/2\sigma_w^2(1+S)}}{\left(2\sigma_w^2(1+S)\right)^n\ \Gamma(n)}ds \\ &= \frac{\Gamma\left(n, \frac{Tz}{a}\right)}{\Gamma(n)} = e^{-Tz/a}\sum_{l=0}^{n-1}\frac{(Tz/a)^l}{l!} \end{aligned} \tag{A.4}$$

Substituting (A.3) and (A.4) in (5), detection probability is:

$$\begin{aligned} P_d &= d\sum_{k=0}^{nr-1} C_k^{rn-1}(-1)^k\left(\frac{I}{b}\right)^{nm-nr+k}\Gamma(nm-nr+k) \\ &\left\{\sum_{l=0}^{n-1}\frac{(T/a)^l}{l!}\int_0^{+\infty} z^{nr-k+l-1}\ e^{-z(1/b+T/a)} - \sum_{j=0}^{nm-nr+k-1}\right. \\ &\left.\frac{(I/b)^j}{j!}\sum_{l=0}^{n-1}\frac{(T/a)^l}{l!}\int_0^{+\infty} z^{nr-1-k+j+l}\ e^{-z(1/c+T/a)}dz\right\} \end{aligned} \tag{A.5}$$

Performing the two integrals in (A.5), leads to:

$$\begin{aligned} P_d &= d\sum_{k=0}^{nr-1} C_k^{rn-1}(-1)^k\left(\frac{I}{b}\right)^{nm-nr+k}\Gamma(nm-nr+k) \\ &\left\{\sum_{l=0}^{n-1}\frac{(T/a)^l}{l!}\frac{\Gamma(nr-k+l)}{(1/b+T/a)^{nr-k+l}} - \sum_{j=0}^{nm-nr+k-1}\frac{(I/b)^j}{j!}\right. \\ &\left.\sum_{l=0}^{n-1}\frac{(T/a)^l}{l!}\frac{\gamma(nr-k+j+l)}{(1/c+T/a)^{nr-k+j+l}}\right\} \end{aligned} \tag{A.6}$$

Replacing a, b, c, and d by their values and performing some simplifications, the detection probability is given in (26).

Appendix B

For incoherently-integrated signals (in the interference free case), the PDF of the sample having the rank k in the ordered sample's set can be obtained by substituting $F_Y(y)$ and $f_Y(y)$ given in (10) in (17):

$$\begin{aligned} f_Z(z) &= kC_k^m\left(\frac{z^{n-1}e^{-z/c}}{c^n\Gamma(n)}\right)\left(e^{-z/c}\sum_{l=0}^{n}\frac{(z/c)^l}{l!}\right)^{m-k} \\ &\quad\times\left(1 - e^{-z/c}\sum_{l=0}^{n}\frac{(z/c)^l}{l!}\right)^{k-1} \end{aligned} \tag{B.1}$$

By developing the last term in (B.1), the PDF of Z will be:

$$\begin{aligned} f_Z(z) &= kC_k^m\left(\frac{z^{n-1}e^{-z/c}}{c^n\Gamma(n)}\right)\sum_{i=0}^{k-1}C_i^{k-1}(-1)^{k-i-1} \\ &\quad\times\left(e^{-z/c}\sum_{l=0}^{n}\frac{(z/c)^l}{l!}\right)^{m-1-i} \end{aligned} \tag{B.2}$$

Developing again the last term in (B.2) leads to:

$$\begin{aligned} f_Z(z) &= \frac{kC_k^m}{\Gamma(n)}\sum_{i=0}^{k-1}C_i^{k-1}(-1)^{k-i-1} \\ &\quad\times\sum_{\left|\vec{j}\right|=m-1-i}\frac{C_{j_0,\ldots,j_{n-1}}^{m-1-i}}{\prod_{t=0}^{n-1}(t!)^{j_t}}\frac{1}{c}\left(\frac{z}{c}\right)^{\sum_{t=0}^{n-1}tj_t+n-1}e^{-(m-i)z/c} \end{aligned} \tag{B.3}$$

Substituting (B.2) and (8) in (5) and performing the following variable change $z = cx$, the detection probability is given by:

$$P_d = \frac{kC_k^m}{\Gamma(n)} \sum_{i=0}^{k-1} C_i^{k-1}(-1)^{k-i-1} \sum_{\left|\vec{j}\right|=m-1-i} \frac{C_{j_0,\ldots,j_{n-1}}^{m-1-i}}{\prod_{t=0}^{n-1}(t!)^{j_t}} \sum_{l=0}^{n} \frac{\left(\frac{T}{1+S}\right)^l}{l!} \int_0^\infty x^{\left(\sum_{t=0}^{n-1} t j_t + l + n - 1\right)} e^{-(m-i+a)x}\, dx \tag{B.4}$$

Computing the integral (B.4) and replacing a by its value, the detection probability is finally given in (27).

Appendix C

For incoherently-integrated signals (in the presence of r interference), the distribution of Z is obtained using the statistics of Y_i and U_i given in (13) and (18):

$$F_Z(z) = \sum_{i=k}^{m} \sum_{j=min(0,i-r)}^{max(i,m-r)} C_j^{m-r} C_{i-j}^{r} \times \left(e^{-z/c} \sum_{l=0}^{n} \frac{(z/c)^l}{l!}\right)^{m-r-j} \left(e^{-z/b} \sum_{l=0}^{n} \frac{(z/b)^l}{l!}\right)^{r-i+j} \times \left(1 - e^{-z/c} \sum_{l=0}^{n} \frac{(z/c)^l}{l!}\right)^{j} \left(1 - e^{-z/b} \sum_{l=0}^{n} \frac{(z/b)^l}{l!}\right)^{i-j} \tag{C.1}$$

Developing the last two terms in (C.1) leads to:

$$F_Z(z) = \sum_{i=k}^{m} \sum_{j=min(0,i-r)}^{max(i,m-r)} C_j^{m-r} C_{i-j}^{r} \sum_{p=0}^{j} \sum_{q=0}^{i-j} C_p^j C_q^{i-j} (-1)^{i-p-q} \times \sum_{\left|\vec{p}\right|=m-r-p} \frac{C_{p_0,\ldots,p_{n-1}}^{m-r-p}}{\prod_{t=0}^{n-1}(t!)^{p_t}} \times \sum_{\left|\vec{q}\right|=r-q} \frac{C_{q_0,\ldots,q_{n-1}}^{r-q}}{\prod_{t=0}^{n-1}(t!)^{q_t}} \left(\frac{z}{c}\right)^{\sum_{t=0}^{n-1} t(p_t+q_t)} e^{-(m-r-p)z/c-(r-q)z/b} \tag{C.2}$$

The detection probability is computed using the following:

$$P_d = \int_0^\infty I(Tz) f_Z(z) dz = -\int_0^\infty \frac{dI(Tz)}{dz} F_Z(z) dz \tag{C.3}$$

with $I(Tz) = e^{-Tz/a} \sum_{l=0}^{n-1} \frac{(Tz/a)^l}{l!}$ and $\frac{dI(Tz)}{dz} = -\frac{(T/a)^n}{\Gamma(n)} z^{n-1} e^{-Tz/a}$. Substituting (C.2) and the derivative of $I(Tz)$ with respect to z in (C.3) and performing the following variable change $z = cx$ leads to:

$$P_d = \frac{\left(\frac{T}{1+S}\right)^n}{\Gamma(n)} \sum_{i=k}^{m} \sum_{j=min(0,i-r)}^{max(i,m-r)} C_j^{m-r} C_{i-j}^{r} \sum_{p=0}^{j} \sum_{q=0}^{i-j} C_p^j C_q^{i-j} (-1)^{i-p-q} \times \sum_{\left|\vec{p}\right|=m-r-p} \frac{C_{p_0,\ldots,p_{n-1}}^{m-r-p}}{\prod_{t=0}^{n-1}(t!)^{p_t}} \sum_{\left|\vec{q}\right|=r-q} \frac{C_{q_0,\ldots,q_{n-1}}^{r-q}}{\prod_{t=0}^{n-1}(t!)^{q_t}} \times \int_0^\infty x^{\left(\sum_{t=0}^{n-1} t(p_t+q_t)+n-1\right)} e^{-\left(m-r-p+\frac{T}{1+S}+\frac{r-q}{1+I}\right)x} dx \tag{C.4}$$

The detection probability is then given in (28).

References

[1] S.M. Kay, Fundamentals of Statistical Signal Processing: Detection Theory, Prentice-Hall, Inc., Upper Saddle River, NJ, USA, 1993.
[2] F. Gini, A. Farina, M. Greco, Selected list of references on radar signal processing, IEEE-Tr-AES 37 (1) (2001).
[3] J. Neyman, E.S. Pearson, On the problem of the most efficient tests of statistical hypotheses, Philos. Trans. R. Soc.London Ser. A 231 (1933) 289–337.
[4] E.L. Lehmann, J.P. Romano, Testing Statistical Hypotheses, Springer Texts in Statistics, third edition, Springer, New York, 2005.
[5] M. Skolnik, Radar Handbook, McGraw-Hill Education, 2008.
[6] H.M. Finn, R.S. Johnson, Adaptive detection mode with threshold control as a function of spatially sampled clutter level estimates, RCA Review 29 (1968) 414–464.
[7] H.E. Bouchlaghem, M. Hamadouche, F. Soltani, K. Baddari, Adaptive clutter-map CFAR detection in distributed sensor networks, AEU - Int. J. Electron. Commun. 70 (2016).
[8] K. Berbra, M. Barkat, F. Gini, M. Greco, P. Stinco, A fast spectrum sensing for CP-OFDM cognitive radio based on adaptive thresholding, Signal Process. 128 (2016) 252–261.
[9] A. Zaimbashi, M.R. Taban, M.M. Nayebi, Y. Norouzi, Weighted order statistic and fuzzy rules CFAR detector for weibull clutter, Signal Process. 88 (3) (2008) 558–570.
[10] Y. Zhou, L.-r. Zhang, Knowledge-aided bayesian radar adaptive detection in heterogeneous environment: GLRT, rao and wald tests, AEU - Int. J. Electron. Commun. 66 (2012).
[11] A. Boudjellal, K. Abed-Meraim, A. Belouchrani, P. Ravier, A new methodology for optimal delay detection in mobile localization context, in: 2013 IEEE International Conference on Acoustics, Speech and Signal Processing (ICASSP), 2013, pp. 6357–6361.
[12] A. Boudjellal, K. Abed-Meraim, A. Belouchrani, P. Ravier, Order-statistics minimum error detector for optimal delay detection in multipath Rayleigh fading channel context, 2013 8th International Workshop on Sys., SP and their App. (WoSSPA), 2013.
[13] P. Grieve, The optimum constant false alarm probability detector for relatively coherent multichannel signals in gaussian noise of unknown power, Inf. Theory IEEE Trans. 23 (1977) 708–721.
[14] M. Barkat, Signal Detection and Estimation, Artech House radar library, Artech House, Norwood, 2005.
[15] B.R. Mahafza, Radar Systems Analysis and Design Using MATLAB, 1st edition, CRC Press, Inc., Boca Raton, FL, USA, 2000.
[16] H. Rohling, Radar CFAR thresholding in clutter and multiple target situations, IEEE-Tr-AES 19 (4) (1983).
[17] M. Shor, N. Levanon, Performances of order statistics CFAR, IEEE-Tr-AES 27 (2) (1991).
[18] C.H. Lim, H.S. Lee, Performance of order-statistics CFAR detector with non-coherent integration in homogeneous situations, IEE Proc. Radar SP 140 (5) (1993) 291–296.
[19] P.P. Gandhi, S.A. Kassam, Optimality of the cell averaging CFAR detector, IEEE Trans. Inf. Theory 40 (4) (1994) 1226–1228.
[20] H.C. Yang, M.S. Alouini, Order Statistics in Wireless Communications: Diversity, Adaptation, and Scheduling in MIMO and OFDM Systems, Cambridge University Press, 2011.
[21] J. Proakis, Digital Communications, 4 edition, McGraw-Hill, 2000.
[22] J.C. Liberti, T.S. Rappaport, Smart Antennas for Wireless Communications: IS-95 and Third Generation CDMA Applications, Prentice Hall PTR, Upper Saddle River, NJ, USA, 1999.
[23] B. Sklar, Digital Communications: Fundamentals and Applications, Prentice-Hall, Inc., Upper Saddle River, NJ, USA, 1988.
[24] J.-M. Chaufray, P. Loubaton, P. Chevalier, Consistent estimation of rayleigh fading channel second-order statistics in the context of the wideband CDMA mode of the UMTS, Signal Process. IEEE Trans. 49 (12) (2001) 3055–3064.
[25] A. Boudjellal, A. Belouchrani, K. Abed-Meraim, 'a new ToAs' CA-CFAR Wiener Rake estimator for downlink mobile positioning in UMTS-FDD system, in: 2011 7th International Workshop on Systems, SP and their Applications (WOSSPA), 2011, pp. 343–347.
[26] 3GPP TR 101.112 UMTS, "Selection procedures for the choice of radio transmission technologies of the UMTS (UMTS 30.03 version 3.1.0)," Tech. Rep., UMTS, Avril 1988.